

FACILITY FORM 802

N65-33650 (ACCESSION NUMBER)	N65-33651 (THRU)
50 (PAGES)	1 (CODE)
CR 64667 (NASA CR OR TMX OR AD NUMBER)	15 (CATEGORY)

July 20, 1965

First Quarterly Report On

Research Study of the Deformation Characteristics of Semi-Brittle Materials Under Ultra-High Hydrostatic Pressures

March 25, 1965 - June 25, 1965

Contract NASW-1199

to

**National Aeronautics and Space Administration
Washington, D.C.**

by

GPO PRICE	\$ _____
CSFTI PRICE(S)	\$ _____
Hard copy (HC)	<u>2.00</u>
Microfiche (MF)	<u>.50</u>

ff 653 July 65

**Pressure Technology Corporation of America
453 Amboy Avenue
Woodbridge, New Jersey**

July 20, 1965

**First Quarterly Report On
Research Study of the Deformation
Characteristics of Semi-Brittle Materials
Under Ultra-High Hydrostatic Pressures**

March 25, 1965 - June 25, 1965

Contract NASW-1199

to

**National Aeronautics and Space Administration
Washington, D.C.**

by

**Pressure Technology Corporation of America
453 Amboy Avenue
Woodbridge, New Jersey**

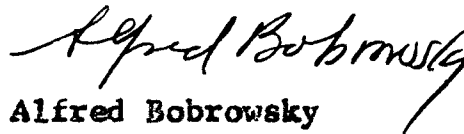
PRESSURE TECHNOLOGY CORPORATION OF AMERICA
453 Amboy Avenue
Woodbridge, New Jersey

July 20, 1965

Gentlemen:

Please find enclosed one copy of the First Quarterly Report entitled "Research Study of the Deformation Characteristics of Semi-Brittle Materials Under Ultra-High Hydrostatic Pressures", produced under contract No. NASW-1199, for the National Aeronautics and Space Administration.

Yours truly,



Alfred Bobrowsky
President

AB:dm
Enc.

TABLE OF CONTENTS

	<u>Page No.</u>
ABSTRACT	
INTRODUCTION	
I. General	1
II. Technical	3
III. Analysis	4
EXPERIMENTAL	9
RESULTS	11
FUTURE WORK	13
REFERENCES	14
ANALYTICAL SUPPLEMENT	15

ABSTRACT

Material has been procured both for super-conductor and tungsten-base alloys. Material has been fabricated into suitable form for conducting tensile tests and fluid-to-fluid extrusions.

Fluid-to-fluid extrusions have been conducted successfully with small reductions on niobium-tin sheathed in metal.

A preliminary investigation has been made of process variables in these fluid-to-fluid extrusion processes.

An analytical study has been made by Dr. Avitzur, consultant, extending a theory on fluid-to-fluid extrusion through conical dies to the case of materials with strain hardening and strain-rate effects.

INTRODUCTION

I. General

It is now generally known that

1. increase in environmental pressure tends to increase ductility of crystalline materials;
2. while under high environmental pressure, poorly-ductile and semi-brittle materials can sometimes be worked;
3. a direct and simple process for working billets of crystalline materials under high fluid pressure is a process first termed fluid-to-fluid extrusion in reference 1.

Previous work along these lines on a variety of materials was performed on a predecessor contract for NASA, Final Report listed as reference 2.

It is realized that the work to be conducted under this contract is of a frontier nature inasmuch as the materials to be worked are considered difficult to deform without fracture at room temperature. For this reason, it was anticipated that investigation would be required not only on the elementary process but also on such variables as die design, lubrication, and the possible necessity of sheathing the material to be worked from contact with the liquid. The effect of liquid in

contact with a metal surface on possible temporary embrittlement of the specimen material was previously noted by Bridgman in several places, but the general effect is usually termed Rabinder effect because of the description of such effects in publications such as reference 3.

It was further realized that it was timely to delve into analysis of the deformation process to a greater extent than had been accomplished in the past. For this reason, the services of Dr. B. Avitzur of Lehigh University were obtained. Dr. Avitzur has published several papers in this general field, some of which are referenced separately in the section concerned with his activity.

Aside from work performed by PTCA for NASA and the Bureau of Weapons of the Department of the Navy (reference 4), there appears to have been no experimentation described in non-geological literature concerned with the controlled deformation of non-ductile materials. References in geological literature pertain to various aspects of deformation of rocks primarily, but it is felt that there has been no contribution in literature during the period of this contract that possesses significance for

the working of semi-brittle metals under consideration.

II. Technical

The introductory material contained in reference 2 described computation of hydrostatic components of stress, and second deviatoric invariant (SDSI). There was also contained therein a description of brittle-ductile transition (BDT) as a function of pressure. This material will not be described again here. It emphasized, however, that the SDSI is used as a criterion for possible onset of plastic flow only for convenience; there is no implication that this criterion for onset of plastic flow is actually more or less suitable than other criteria for the materials to be investigated in this project. There is considerable evidence throughout literature that SDSI may be suited for use with certain materials but is unsuited for use with other materials (reference 5).

The major addition to the previous concepts harks back to earlier thoughts on flow and fracture stresses in materials. This concept was usually stated in terms of the variation of flow and fracture stresses as a function of temperature. It was indicated that at higher temperature the fracture stress exceeded the flow stress with the result that the material was ductile. At

lower temperatures, the reverse was true so that the material fractured before it had a chance to flow. The same sort of behavior occurs with pressure replacing temperature as a variable. This has been well documented in literature as in reference 6. In references such as reference 6, this behavior is depicted as a variation of ductility in tensile tests as a function of environmental pressure. Below the brittle-ductile transition pressure (BDTP), the flow stress exceeds the fracture stress so that fracture is brittle; the reverse occurs above the BDTP.

Semi-brittle materials are materials whose flow and fracture stresses are nearly equal at room temperature and atmospheric pressure. If the brittle condition persists for a considerable increase in environmental pressure and/or temperature, the material is more nearly termed brittle.

III. Analysis

This analysis represents preliminary thinking on macroscopic considerations at the BDT.

The late Dr. P.W. Bridgman in his book on plastic flow (reference 7) found it difficult to see how a ten-

side fracture could be initiated in the interior of a tensile-test specimen if all principal stresses remained compressive. This thought appears to be correct on an intuitive basis because rupture implies the separation of planes of atoms such that work must be performed against the existing pressure in order to effect the fracture.

Dr. A.H. Cottrell at the 1959 Swampscott Symposium on Fracture (reference 8) referenced unpublished research by D. Hull and D.E. Rimmer of the Atomic Energy Research Establishment to the effect that no internal cracks were produced in a tensile specimen of a certain material if the tensile stress in the specimen were exceeded by a superposed environmental hydrostatic pressure.

It thus appears possible that a material will remain brittle as environmental pressure increases until a sufficiently high pressure is attained at which point the fracture stress exceeds the flow stress and the material is now termed ductile. Flow stress is defined here as by Bridgman, namely, as the uniaxial stress remaining after the other two principal stresses have been reduced to zero by subtracting appropriate hydrostatic stress. So long as the material is in a brittle state, and so long as the environmental pressure exceeds the fracture strength, the brittle material can never be fractured in tension.

After a material is in the ductile state, it will fracture after having been strained sufficiently. The fracture will occur for two reasons:

- (a) As the material is strained, it work hardens and thus becomes a new material with a different and possibly reversed relationship between flow and fracture stresses.
- (b) Tensile instability may occur in the form of a neck in the specimen. As Bridgman has shown, this neck is responsible for a superposed hydrostatic tension being generated within the body of the tensile specimen, thus tending to offset the environmental pressure.

It thus appears that the BDTP in tension is a good measure of the fracture stress at the BDTP. Inasmuch as the fracture and flow stresses are nearly equal at the BDTP, the environmental pressure thus measures the flow stress there, also.

As environmental pressure rises higher than the BDTP, the flow stress in general tends to rise at least for a while. This may actually be a manifestation of inhomogeneity of physical properties in the specimen material. Some portions of the specimen material may actually have a high flow stress typical of the material in a more fully ductile condition, but other portions of

the material in the vicinity of the BDEP may not yet be in a ductile state. The average behavior of the various portions of the bulk material of the specimen thus yields some amount of ductility, but fracture of some portions of the bulk material will cause the macroscopic nominal stress to appear lower than that of fully ductile material.

For these reasons, it would appear to be important to employ an environmental pressure not merely slightly above the BDEP but probably well above that value of pressure. In this way, it should be possible to tend to cause most of the bulk material of the specimen to behave in a fully ductile manner.

Another practical implication of the relation between flow and fracture stresses near the BDT is that materials worked under pressure can be bettered more in physical properties than might ordinarily be thought to be the case. For example, copper that has been hard drawn by a wire drawing process rarely exceeds Rockwell B55 in hardness. At that point the copper is very brittle. When the material is worked at 200,000 psi pressure, however, an unprecedented hardness of Rockwell B75 can be obtained. This copper is nevertheless extremely malleable (reference 9). Although the material

drawn by conventional processes possessed hardness of RB55, its tensile strength was actually somewhat lower than might be obtained from an extrapolation of hardness vs. strength for the copper. This occurs because the material in tension is relatively brittle so that the fracture stress tends to predominate in its tensile behavior. In a hardness test, the compressive component of stress tends to make the material somewhat more ductile to the indenter so that the compressive strength of the material in a hardness test would ordinarily exceed the tensile strength as measured by conventional tensile tests. The Rockwell B 75, however, is fully ductile and consequently all material in the cross section tends to support flow stress prior to fracture so that the strength of the Rockwell B75/^{material}worked in this manner should be considerably higher than would be thought from the strength-hardness relation of Rockwell B55 material drawn by conventional means.

EXPERIMENTAL

The processes to be employed are tensile tests under pressure and fluid-to-fluid extrusion of metals. These processes as performed by PTCA have been described many times in literature, as for example reference 2.

A major deviation from the tensile tests previously performed are that it may be necessary to modify the tensile specimen size and/or shape in view of the limited availability of specimen material of semi-conducting metal.

Materials obtained to date have been niobium-tin from the Superior Tube Company, and tungsten-base alloy from the sponsor.

The outside diameter of the niobium-tin sheath was 0.143". The sheath is actually a double sheath, according to information supplied by Superior Tube Company. The outer sheath is Monel and the inner sheath is niobium. A core of niobium-tin exists within. This material was supplied with the core in powder form. The niobium-tin alloy was made according to instructions from Superior Tube Company, through the assistance of the Research and Development Division of Engelhard Industries who kindly vacuum heat-treated the material. Although some of the

material at the ends of the tube was exposed during the heating, no melting of the tin was apparent.

The tungsten-base material was lightly machined and revealed some cracks. It is proposed to continue to work with this material despite the presence of cracks unless it appears that the cracks will greatly hamper adequate performance of the material during working.

Portions of the niobium-tin wire were cut into billets approximately 1/2" long. The sheath was nosed to a 40° included angle, and the billet was placed in a 40° die. A small amount of beeswax was employed as the lubricant, and the extrusion liquid was an SAE 10 Pennsylvania-grade oil.

RESULTS

Results are still preliminary. Initial small reductions (about 10 to 20%) of the sheathed niobium-tin material, ends exposed to the liquid environment, showed that the niobium-tin material cracked after fluid extrusion into atmospheric pressure. A back pressure in the order of 80,000 psi, however, appeared to be adequate to suppress cracking of the niobium-tin for 11% reduction. A second extrusion of the previously extruded material into the same back pressure resulted in very fine cracking. It should be noted that the fluid-to-fluid extrusion process tends to cause the Monel sheath to separate from the niobium sheath so that die pressure on the core of the material may be relatively uneven. It may be necessary to remove the Monel sheath in future fluid-to-fluid extrusions.

The ends of the fluid-to-fluid extruded specimens indicated that the niobium sheath tends to deform more readily than the niobium-tin core. The result is a cup-like appearance at both ends of the fluid-to-fluid extruded specimen that has not been nosed prior to extrusion. It should be noted that although nosed billets

were employed during part of these runs, it was found that square ended billets could be employed successfully in fluid-to-fluid extrusion, as PTCA has done previously with other materials. Whether a billet is nosed or not is of no major consequence if long lengths are in question since lack of nosing simply increases the yield of fully reduced material, inasmuch as material in the nose of the specimen is not fully reduced. Noses may or may not be employed in the current work, with no implication that lack of a nose is a material advantage for niobium-tin which presumably would be desired in extremely long length for ultimate utilization.

FUTURE WORK

Additional tungsten-base material is being sought from the sponsor to supplement the material already on hand. Attempts will be made to obtain superconducting material of other composition than niobium-tin. Such attempts have already been made with regard to niobium-zirconium and vanadium-gallium alloys, but no supplier of either samples or considerable lengths has been found.

Tensile test procedures will be modified to make use of non-standard samples. Investigation will continue on both types of materials.

REFERENCES

1. SCORSE, JERRY: "Fluid-to-Fluid Extrusion Developed For Cold-Forming Refractory Metals", Metalworking News, October 29, 1962, Vol. 3, Whole No. 108.
2. BOBROWSKY, A.; and STACK, E.A.: "Final Report on an Investigation of Fluid Extrusion of Metals", Contract NASw-742 to National Aeronautics and Space Administration, Washington, D.C., February 27, 1965.
3. LIKHTMAN, V.I.; REBINDER, P.A.; and KARPENKO, G.B.: "Effect of Surfact-Active Medium on the Deformation of Metals", published Moscow 1954, available in translation as published by H.M.S.O., London 1958.
4. BOBROWSKY, A.: "An Investigation of Be and W Altered by High-Pressure Deformation", progress reports 1, 2, 3, 4, and 5, prepared under Navy, Bureau of Naval Weapons, Contract No. NOW 64-0180-c.
5. BOBROWSKY, A.; and STACK, E.A.: "Research on Hydrostatic Extrusion of the TZM Alloy at Ambient Temperature", Technical Documentary Report No. ML-TDR-64-205, June 1964 prepared for AF Materials Laboratory, Research and Technology Division, Air Force Systems Command, Wright-Patterson Air Force Base, Ohio, Project No. 7351, Task No. 735103, pgs 57 - 60.
6. BOBROWSKY, A.; and STACK, E.A.: "A Study to Determine the Deformation Characteristics of Beryllium and Tungsten Under Conditions of High Hydrostatic Pressure", Final report prepared Under Navy, Bureau of Weapons, Contract No. N 600 (19) 59430, September 1963.
7. BRIDGMAN, P.W.: "Studies in Large Plastic Flow and Fracture", McGraw-Hill Book Company, Inc., New York, 1952.
8. AVERBACH, B.L.; FELBECK, D.K.; HAHN, G.T.; and THOMAS, D.A., Editors: "Fracture", published by John Wiley & Sons, Inc., 1959.
9. FUCHS, F.J., JR.: "Production Metal Forming with Hydrostatic Pressure", ASME Paper No. 65-PROD-17, June 1965.

ANALYTICAL SUPPLEMENT

N 65-33651

Accounting for Strain Hardening
And Strain Rate Effects
In Fluid-to-Fluid (Hydrostatic) Extrusion

by

Dr. B. Avitzur
Lehigh University
Bethlehem, Pennsylvania

This material is in preliminary draft form in this progress report.

ACCOUNTING FOR STRAIN HARDENING AND STRAIN RATE
EFFECTS IN FLUID-TO-FLUID (HYDROSTATIC) EXTRUSION

ABSTRACT

33651

A kinematically admissible velocity field and the resulting extrusion pressure characteristics, as solved earlier for non-strain hardening materials, are first presented again. Effective strain rates and effective strains are computed, and the effects of strain hardening and strain rate sensitivity on the process are evaluated.

Author

NOMENCLATURE

J^*	upper bound on power
L	length of land of die
m	shear factor
n	exponent for strain hardening
P_a	receiving chamber pressure
P_b	extrusion pressure
R	radial distance
R_f	final radius
R_o	original radius
r, θ, φ	axes of spherical coordinate system
S	flow stress at unit strain rate
S_t	surface over which tractions are prescribed
S_r	surface of velocity discontinuity
T	prescribed applied surface tractions
t	time
U_r, U_θ, U_φ	components of the velocity vector in a spherical coordinate system
V	volume
\dot{V}	volume rate
v	velocity
v_f	final velocity
v_o	initial velocity

NOMENCLATURE (Cont'd)

\dot{W}	power
\dot{W}_b	power supplied by extrusion pressure
\dot{W}_a	power to overcome receiving chamber pressure
\dot{W}_i	internal power of deformation
$W_{S_{12}}$	Shear power as over surfaces Γ_1 and Γ_2
W_{S_3} W_{S_4}	Friction power loss over surfaces Γ_3 and Γ_4
α	cone semi-angle of die
α_{opt}	optimal die angle
Γ	boundary of velocity discontinuity
Δv	velocity discontinuity
ϵ	engineering strain
$\dot{\epsilon}$	strain rate
ϵ_{ij}	components of strain-rate tensor
μ	Coulomb coefficient of friction
σ_o	yield limit in uniaxial tensile test
τ	shear stress
ϕ	effective strain
$\dot{\phi}$	effective strain rate
$\bar{\phi}$	average effective strain
$\bar{\dot{\phi}}$	average effective strain rate
ϕ_o	ideal effective strain

NOMENCLATURE (Cont'd)

subscripts

1, 2, 3, 4

surfaces as shown in figure 2

KINEMATICALLY ADMISSIBLE VELOCITY FIELD

As presented in previous studies (ref. 1 and 2) of the process, the assumption is made that the die is a rigid body of the geometry shown in figure 1. A kinematically admissible velocity field is described in figure 2. The wire is divided into three regions in which the velocity field is continuous. In zones I and III, the velocity is uniform and has only an axial component. In zone I the velocity is v_0 while in zone III the velocity is v_f .

Due to volume constancy,

$$v_0 = v_f \left(\frac{R_f}{R_0} \right)^2 \quad (1)$$

In zone II the velocity is directed towards the apex (O) of the cone, with cylindrical symmetry.

In the spherical coordinated $s (r, \varphi, \theta)$, the velocity components are:

$$\left. \begin{aligned} \dot{U}_r = v &= -v_f r_f^2 \frac{\cos \theta}{r^2} \\ \dot{U}_\theta = \dot{U}_\varphi &= 0 \end{aligned} \right\} \quad (2)$$

Across the boundaries Γ_1 and Γ_2 the components of velocity normal to the surfaces Γ_1 and Γ_2 are continuous.

There exist velocity discontinuities, parallel to these surfaces, of magnitudes:

$$\text{along } \Gamma_1 \quad \Delta v = v_f \sin \theta; \quad (3)$$

$$\text{along } \Gamma_2 \quad \Delta v = v_o \sin \theta. \quad (4)$$

Since the die is at rest, the velocity discontinuities along surfaces Γ_3 and Γ_4 are:

$$\text{along } \Gamma_3 \quad \Delta v = v_f r_f \frac{\cos \theta}{r_2} \quad (5)$$

$$\text{along } \Gamma_4 \quad \Delta v = v_f. \quad (6)$$

POWER BALANCE

The upper bound theorem as presented by Prager on page 237 of reference 3, slightly adjusted for this case, reads

$$J^* = \frac{2}{\sqrt{3}} \int_V \sigma_o \sqrt{\frac{1}{2} \dot{\epsilon}_{ij} \dot{\epsilon}_{ij}} dV + \int_{S_r} \tau |\Delta v| dS - \int_{S_t} \tau_i v_i dS. \quad (7)$$

The individual terms are presented next for fluid-to-fluid (hydrostatic) extrusion.

Supplied power,

$$J^* = \pi v_o R_o^2 p_b = \pi v_f R_f^2 p_b. \quad (8)$$

INTERNAL POWER OF DEFORMATION

The strain rates as devised in reference 1 from the velocity field of equation (1) are

$$\left. \begin{aligned} \dot{\epsilon}_{rr} &= -2\dot{\epsilon}_{\theta\theta} - 2\dot{\epsilon}_{\varphi\varphi} = 2v_f r_f^2 \frac{\cos \theta}{r^3} \\ \dot{\epsilon}_{r\theta} &= \frac{1}{2} v_f r_f^2 \frac{\sin \theta}{r^3} \\ \dot{\epsilon}_{\theta\varphi} &= \dot{\epsilon}_{r\varphi} = 0 \end{aligned} \right\} \quad (9)$$

Substituting the terms into the volume integral and assuming a constant value for the flow stress σ_0 , leads to:

$$\dot{W}_i = 2\pi\sigma_0 v_f R_f^2 f(\alpha) \ln \frac{R_0}{R_f}, \quad (10)$$

where

$$f(\alpha) = \frac{1}{\sin^2 \alpha} \left\{ 1 - (\cos \alpha) \sqrt{1 - \frac{11}{12} \sin^2 \alpha} + \frac{1}{\sqrt{11/12}} \ln \frac{1 + \sqrt{\frac{11}{12}}}{\sqrt{\frac{11}{12}} \cos \alpha + \sqrt{1 - \frac{11}{12} \sin^2 \alpha}} \right\};$$

the function will be shown to measure the relative average effective strain.

FRICITION AND SHEAR LOSSES

Over the surfaces of velocity discontinuities shear stress cannot exceed the value of

$$\tau = \frac{\sigma_0}{\sqrt{3}}. \quad (11)$$

Shear losses over surfaces Γ_1 and Γ_2 become

$$\dot{W}_{S_{12}} = \int_{\Gamma_1, \Gamma_2} \tau \cdot \Delta v \cdot ds = 4\pi r_f^2 v_f \frac{\sigma_0}{\sqrt{3}} \int_{\theta=0}^{\alpha} \sin^2 \theta d\theta \quad (12)$$

$$\therefore \dot{W}_{S_{12}} = \frac{2}{\sqrt{3}} \sigma_0 \pi v_f R_f^2 \left[\frac{\alpha}{\sin^2 \alpha} - \cot \alpha \right]. \quad (13)$$

When friction is assumed to obey the constant shear factor law

$$\tau = m \frac{\sigma_0}{\sqrt{3}}, \quad (14)$$

friction losses become:

$$\dot{W}_{S_3} = \int_{\Gamma_3} \tau \Delta v ds = 2\pi v_f R_f^2 \cot \alpha \cdot m \frac{\sigma_0}{\sqrt{3}} \int_{R_f}^{R_0} \frac{dR}{R} \quad (15)$$

$$\dot{W}_{S_3} = \frac{2}{\sqrt{3}} \sigma_0 m \pi v_f R_f^2 \cot \alpha \ln \frac{R_0}{R_f} \quad (16a)$$

and

$$\dot{W}_{S_4} = \frac{2}{\sqrt{3}} \sigma_0 m \pi v_f R_f^2 \frac{L}{R_f}. \quad (17a)$$

When friction is assumed to obey Coulomb's law of friction

$$\tau = \mu p, \quad (18)$$

friction losses become:

$$\dot{W}_{S_3} = 2\mu \pi v_f R_f^2 (\cot \alpha) \left[1 - \frac{p_a}{\sigma_0} + \ln \frac{R_0}{R_f} \right] \ln \frac{R_0}{R_f} \quad (16b)$$

and

$$\dot{W}_{S_4} = 2\mu \left(1 - \frac{p_a}{\sigma_0} \right) \frac{L}{R_f} \quad (17b)$$

POWER TO OVERCOME PRESSURE AT THE RECEIVING CHAMBER

To push the billet against the pressure at the receiving chamber, the power required is:

$$\dot{W}_a = \int_{S_t} \tau_i v_i dS = \pi v_f R_f^2 p_a \quad (19)$$

POWER BALANCE

When the values of the individual terms of equations (10), (13), (16), (17) and (19) are substituted into equation (7), the resulting required extrusion pressure for non-strain-hardening materials becomes:

a) For the assumption of a constant friction factor;

$$\frac{p_b}{\sigma_0} = \frac{p_a}{\sigma_0} + 2f(\alpha) \ln \frac{R_0}{R_f} + \frac{2}{\sqrt{3}} \left\{ \frac{L}{\sin^2 \alpha} - \cot \alpha + m \left[(\cot \alpha) \ln \frac{R_0}{R_f} + \frac{L}{R_f} \right] \right\}; \quad (20a)$$

b) For the assumption of Coulomb friction

$$\frac{p_b}{\sigma_0} = \frac{p_a}{\sigma_0} + 2f(\alpha) \ln \frac{R_0}{R_f} + \frac{2}{\sqrt{3}} \left(\frac{L}{\sin^2 \alpha} - \cot \alpha \right) + 2\mu \left\{ (\cot \alpha) \left[1 + \frac{p_a}{\sigma_0} + \ln \frac{R_0}{R_f} \right] + \left(1 + \frac{p_a}{\sigma_0} \right) \frac{L}{R_f} \right\} \quad (20b)$$

where $f(\alpha)$ is defined in equation (10) and is presented in table 1 for $0 \leq \alpha \leq 90^\circ$ in increments of one degree for ϵ .

The extrusion pressure is expended to:

1. overcome the pressure at the low pressure chamber,
2. overcome the resistance of the material to internal deformation -- part of which is called the ideal power of deformation.

$$\dot{W}_{ideal} = \pi v_f R_f^2 \ln \frac{R_0}{R_f}. \quad (21)$$

The other part provides some of the excess power of deformation

$$\dot{W}_{redundant} = \pi v_f R_f^2 [f(\alpha) - 1] \ln \frac{R_0}{R_f}. \quad (22)$$

3. The other part of the redundant power of deformation is the shear over surfaces Γ_1 and Γ_2 , given by equation (12).
4. Friction losses over the surface of the die are given by equations (16) and (17).

OPTIMAL CONE ANGLE

Friction losses are very high for very small cone angles, dropping to zero for a square die. Redundant power is zero with zero cone angle and increases as the cone angle increases. The combined effect on the pressure is

given in figure 3, showing an optimal cone angle, which minimizes the required extrusion pressure, see references 4, 5, and 6.

The value of the optimal cone angle is approximated (references 1, 2, and 7) by:

a) For the assumption of a constant friction factor

$$\alpha_{opt} = \sqrt{\frac{3}{2} m \ln \frac{R_0}{R_f}} ; \quad (23a)$$

b) For Coulomb friction

$$\alpha_{opt} = \sqrt{\frac{3}{2} \sqrt{3} \mu \left(1 + \frac{P_2}{\sigma_0} + \ln \frac{R_0}{R_f} \right) \ln \frac{R_0}{R_f}} \quad (23b)$$

EFFECTIVE STRAIN RATES AND EFFECTIVE STRAIN

To account for the effects of strain hardening and strain-rate sensitivity, the effective strain rates and effective strains are to be evaluated.

The effective strain rate is an accepted measure of the combined effect of the components of strain rates. It is a means of comparison between different modes of straining. The effective strain rate is defined by:

$$\dot{\phi} = \frac{2}{\sqrt{3}} \sqrt{\frac{1}{2} \dot{\epsilon}_{ij} \dot{\epsilon}_{ij}} \quad (24)$$

Substituting the values of the strain rates from equation (9) into equation (24) leads to

$$\dot{\phi} = 2v_f r_f^2 \frac{1}{r^3} \sqrt{1 - \frac{11}{12} \sin^2 \theta} . \quad (25)$$

The effective strain rate is a function of r and θ . Of interest is the total strain after each material point passes through the die. Since the material moves on radial lines with constant θ , the total strain is computed by integration with respect to r as follows.

$$\phi = \int_{t=0}^t \dot{\phi} dt . \quad (26)$$

$$\text{Since } dr = v dt$$

(27)

it follows by equation (2) for v that

$$dt = \frac{dr}{v} = \frac{r^2 dr}{v_f r_f^2 \cos \theta} . \quad (28)$$

Substitution of equation (25) and (28) into equation (26) leads to

$$\phi = -2 \frac{\sqrt{1 - \frac{11}{12} \sin^2 \theta}}{\cos \theta} \int_{r=r_0}^r \frac{dr}{r} = 2 \frac{\sqrt{1 - \frac{11}{12} \sin^2 \theta}}{\cos \theta} \ln \frac{R_0}{R} . \quad (29)$$

The effective strain is highest at the surface of the die (=). Both an increase in reduction and an increase in entrance cone angle cause an increase in the effective strain.

The cumulative effective strain of the extruded product, found when $r = r_f$, is

$$\phi = 2 \frac{\sqrt{1 - \frac{11}{12} \sin^2 \theta}}{\cos \theta} \ln \frac{R_0}{R_f}. \quad (30)$$

At $r = r_f$ the substitution

$$\sin \theta = \frac{R}{r_f} = \frac{R}{R_f} \sin \alpha \quad (31)$$

leads to

$$\phi = 2 \frac{\sqrt{1 - \frac{11}{12} \left(\frac{R}{R_f}\right)^2 \sin^2 \alpha}}{\sqrt{1 - \left(\frac{R}{R_f}\right)^2 \sin^2 \alpha}} \ln \frac{R_0}{R_f}. \quad (32)$$

When the cone angle α approaches zero, the effective strain of the product becomes

$$\phi_0 = 2 \ln \frac{R_0}{R_f}. \quad (33)$$

This is the definition of the ideal effective strain when no distortion occurs. The amount of strain at the center ($R = 0$) is the same as at the surface ($R = R_f$). Let the relative effective strain be defined as follows:

$$\frac{\phi}{\phi_0} = \frac{\sqrt{1 - \frac{11}{12} \left(\frac{R}{R_f}\right)^2 \sin^2 \alpha}}{\sqrt{1 - \left(\frac{R}{R_f}\right)^2 \sin^2 \alpha}} \quad (34)$$

Equation (34) is described in figure 4 where the relative effective strain for various cone angles is plotted vs. the distance from the center of the rod.

The following observations are confirmed:

1. The larger the reduction, the larger is the effective strain.
2. The effective strain increases from the center of the product towards the outer surface. For small cone angles the effective strain is almost constant.
3. Large cone angles cause an increase in the effective strain. This effect is most pronounced at the surface.

For strain hardening materials one concludes that large reductions, large cone angles, and increased distance from the axis of symmetry all cause an increase in the effective strain and, hence, higher hardness, strength, and brittleness. Results of microhardness distribution tests are shown in figure of reference 8 ^{taken from} and figure 22 [^] of reference 6. See also references 9 and 10.

A practical value for an average effective total radius is

$$\bar{\phi} = \frac{2\pi \int_{R=0}^{R_f} R \phi dR}{\pi R_f^2} = 4 \left(\ln \frac{R_0}{R_f} \right) \int_{R=0}^{R_f} \left(\frac{R}{R_f} \right) \frac{\sqrt{1 - \frac{11}{12} \left(\frac{R}{R_f} \right)^2 \sin^2 \alpha}}{\sqrt{1 - \left(\frac{R}{R_f} \right)^2 \sin^2 \alpha}} d \left(\frac{R}{R_f} \right); \quad (35)$$

substituting

$$\left(\frac{R}{R_f} \right)^2 \sin^2 \alpha = y; \quad 2 \left(\frac{R}{R_f} \right) d \left(\frac{R}{R_f} \right) = \frac{dy}{\sin^2 \alpha}; \quad (36)$$

$$\bar{\phi} = \frac{2 \ln \left(\frac{R_0}{R_f} \right)}{\sin^2 \alpha} \int \frac{\sqrt{1 - \frac{11}{12} y}}{\sqrt{1 - y}} dy \quad (37)$$

$$\bar{\phi} = \frac{2 \ln \left(\frac{R_0}{R_f} \right)}{\sin^2 \alpha} \left(-\sqrt{1-y} \sqrt{1 - \frac{11}{12} y} + \frac{1}{\sqrt{11 \cdot 12}} \ln \left| \sqrt{\frac{11}{12} (1-y)} - \sqrt{1 - \frac{11}{12} y} \right| \right) \quad (38)$$

$$\begin{aligned} \bar{\phi} = \frac{2 \ln \left(\frac{R_0}{R_f} \right)}{\sin^2 \alpha} & \left(-\sqrt{1 - \left(\frac{R}{R_f} \right)^2 \sin^2 \alpha} \sqrt{1 - \frac{11}{12} \left(\frac{R}{R_f} \right)^2 \sin^2 \alpha} + \right. \\ & \left. + \frac{1}{\sqrt{11 \cdot 12}} \ln \left| \sqrt{\frac{11}{12} \left[1 - \left(\frac{R}{R_f} \right)^2 \sin^2 \alpha \right]} - \sqrt{1 - \frac{11}{12} \left(\frac{R}{R_f} \right)^2 \sin^2 \alpha} \right| \right) \Bigg|_{R=0}^{R=R_f} \quad (39) \end{aligned}$$

$$\bar{\phi} = \frac{2 \ln \frac{R_0}{R_f}}{\sin^2 \alpha} \left\{ 1 - \sqrt{1 - \sin^2 \alpha} \sqrt{1 - \frac{11}{12} \sin^2 \alpha} - \frac{1}{\sqrt{11 \cdot 12}} \ln \frac{\sqrt{\frac{11}{12}} - 1}{\sqrt{\frac{11}{12}} \sqrt{1 - \sin^2 \alpha} - \sqrt{1 - \frac{11}{12} \sin^2 \alpha}} \right\}; \quad (40)$$

with proper manipulation

$$\left\{ \begin{aligned} \bar{\phi} &= \frac{2 \ln \frac{R_0}{R_f}}{\sin^2 \alpha} \left\{ 1 - \cos \alpha \sqrt{1 - \frac{11}{12} \sin^2 \alpha} + \frac{1}{\sqrt{11/12}} \ln \frac{1 + \sqrt{11/12}}{\sqrt{1 - \frac{11}{12} \sin^2 \alpha} + \sqrt{\frac{11}{12} \cos^2 \alpha}} \right\} \\ \bar{\phi} &= 2 f(\alpha) \ln \frac{R_0}{R_f} . \end{aligned} \right. \quad (41)$$

This expression neglects the strain accumulated over the surfaces 1 and 2 as shear.

The relative average effective strain is expressed by the function

$$\frac{\bar{\phi}}{\phi} = f(\alpha), \quad (42)$$

where $f(\alpha)$ is tabulated in table 1.

One notices that for large cone angles the effective strain rate at the surface is increasing steeply. When $\alpha = 90^\circ$, the effective strain at the surface approaches infinity (see equation (34) and figure 4). In spite of that behavior (because the strain at the surface is only skin deep), the average effective strain changes only moderately with α . (see table 1).

A practical value for an average effective strain rate is

$$\bar{\dot{\phi}} = \frac{1}{V} \int_V \dot{\phi} dV = \frac{1}{V} \frac{2}{\sqrt{3}} \int_V \sqrt{\frac{1}{2} \dot{\epsilon}_{ij} \dot{\epsilon}_{ij}} dV. \quad (43)$$

Since the volume V is the volume of the deformation zone II,

$$V = \frac{2}{3} \pi \frac{1 - \cos \alpha}{\sin^3 \alpha} (R_0^3 - R_f^3) = \frac{2}{3} \pi \frac{R_0^3 - R_f^3}{(1 + \cos \alpha) \sin \alpha}, \quad (44)$$

substitution of the values of the strain rates of equation (9) into equation (43) and performing the integration results in

$$\bar{\dot{\phi}} = 2 \frac{\dot{V}}{V} f(\alpha) \ln \frac{R_0}{R_f}, \quad (45)$$

where V is given by equation (44), $f(\alpha)$ by equation (10) and

$$\dot{V} = \pi v_f R_f^2. \quad (46)$$

The relative average effective strain rate becomes

$$\frac{\bar{\dot{\phi}}}{\dot{\phi}_0} = \frac{3}{2} \frac{v_f}{R_f} \frac{(1 + \cos \alpha) \sin \alpha f(\alpha)}{\left(\frac{R_0}{R_f}\right)^3 - 1}. \quad (47)$$

The expression

$$\frac{R_f}{v_f} \cdot \frac{\bar{\dot{\phi}}}{\dot{\phi}_0} = \frac{3}{2} \frac{(1 + \cos \alpha) \sin \alpha f(\alpha)}{\left(\frac{R_0}{R_f}\right)^3 - 1} \quad (48)$$

is described in figure 5.

If the final radius (R_f) and exit velocity (v_f) are kept constant, an increase in reduction causes a decrease in the average effective strain rate. An increase in cone angle causes initial increase in the average effective strain rates. But as the cone angle approaches 90° , and if a dead zone does not form, the reverse happens. Noticing that the velocity (equation (2)) and the effective strain rate (equation (25)) drop at the surface for large angles, this is not surprising.

STRAIN HARDENING MATERIALS

As a first approximation for the relative extrusion pressure, Equation (20a) or equation (20b) can be used, where the flow stress σ_o is taken from tensile test data. The average effective strain of the product is computed by equation (41). If the original material was in the annealed state, its effective strain was $\bar{\phi} = 0$. An average value between the billet and the product becomes

$$\bar{\phi}_a = f(\lambda) \ln \frac{R_o}{R_f} . \quad (49)$$

The stress-strain curve will provide the flow stress when the effective strain in uniaxial tension is

$$\bar{\phi}_o = 2 \ln \frac{R_o}{R_f} = \ln \left(\frac{R_o}{R_f} \right)^2 = \ln \left(\frac{L}{L_o} \right) = \ln (1 + \epsilon), \quad (50)$$

where ϵ is the engineering strain.

STRAIN RATE SENSITIVITY

When a material is deformed at a temperature above its recrystallization temperature, it does not strain-harden. It is however sensitive to the rate of straining or to the strain rates. For most commercial metals the recrystallization temperature is above room temperature; (recrystallization temperature varies with composition and for the same composition varies with the amount of cold work and the time allowed.)

For some materials the recrystallization temperature is below room temperature, for example, as for lead. Above the recrystallization temperature strain hardening vanishes. However the material is then very sensitive to the strain rates. For example, from figure 2b of reference 11, the flow stress for commercially pure lead was found to be

$$\sigma_0 = 2457 \dot{\phi}^{0.12} \quad (51)$$

As a first approximation for the relative extrusion pressure, equation (20a) can be used, where the flow stress is taken from tensile-test data plotted for material such as in figure 2b of reference 11, or translated in an equation of the form of equation (51).

For strain-rate-sensitive materials, the flow stress is expressed as

$$\sigma_o = s \dot{\phi}^n, \quad (52)$$

where s and n are constants of the material. When $n = 0$ the material is not sensitive to strain rates. Increasing values of n indicate an increase in strain-rate sensitivity. The value of s is the flow stress of the material for a unit ($1/1$ /unit time) strain rate.

Lead, for example, based on Yang's (reference 11) graph, has recommended values of $s = 2457$ and $n = 0.12$. (See reference 12). The effective strain rate can be taken as the average recommended by equation (47).

An example of the increased extrusion pressure for lead with an increase in extrusion speed is shown by a recorded experiment in figure 6 (reference 12).

TABLE 1

1	1,00001	0,011636	31	1,00672	0,37539	61	1,03603	0,83746
2	1,00003	0,023275	32	1,00721	0,38854	62	1,03784	0,85632
3	1,00006	0,034920	33	1,00772	0,40180	63	1,03974	0,87549
4	1,00010	0,046573	34	1,00825	0,41516	64	1,04174	0,89500
5	1,00016	0,058237	35	1,0081	0,42864	65	1,04384	0,91484
6	1,00023	0,069915	36	1,00930	0,44224	66	1,04605	0,93503
7	1,00031	0,081611	37	1,01000	0,45596	67	1,04838	0,95559
8	1,00041	0,093327	38	1,01063	0,46981	68	1,05082	0,97655
9	1,00052	0,10507	39	1,01129	0,48380	69	1,05340	0,99787
10	1,00064	0,11683	40	1,01198	0,49792	70	1,05613	1,01961
11	1,00078	0,12862	41	1,01270	0,51218	71	1,05900	1,04173
12	1,00093	0,14045	42	1,01345	0,52660	72	1,06204	1,06435
13	1,00109	0,15231	43	1,01423	0,54117	73	1,06526	1,08743
14	1,00127	0,16421	44	1,01505	0,55590	74	1,06867	1,11092
15	1,00146	0,17614	45	1,01590	0,57080	75	1,07228	1,13501
16	1,00167	0,18813	46	1,01679	0,58587	76	1,07611	1,15959
17	1,00189	0,20016	47	1,01772	0,60111	77	1,08018	1,18467
18	1,00212	0,21223	48	1,01869	0,61655	78	1,08451	1,21031
19	1,00237	0,22437	49	1,01970	0,63217	79	1,08912	1,23653
20	1,00264	0,23656	50	1,02075	0,64800	80	1,09404	1,26333
21	1,00292	0,24881	51	1,02185	0,66403	81	1,09928	1,29081
22	1,00322	0,26112	52	1,02300	0,68027	82	1,10488	1,31897
23	1,00354	0,27350	53	1,02420	0,69674	83	1,11087	1,34781
24	1,00387	0,28595	54	1,02546	0,71344	84	1,11727	1,37731
25	1,00422	0,29848	55	1,02677	0,73037	85	1,12413	1,40741
26	1,00459	0,31108	56	1,02814	0,74755	86	1,13148	1,43811
27	1,00498	0,32377	57	1,02958	0,76498	87	1,13935	1,47021
28	1,00538	0,33653	58	1,03108	0,78268	88	1,14780	1,50281
29	1,00581	0,34939	59	1,03265	0,80066	89	1,15687	1,53681
30	1,00625	0,36234	60	1,03430	0,81891	90	1,16660	1,57081

REFERENCES

1. AVITZUR, B., "Analysis of Wire Drawing and Extrusion Through Conical Dies of Large Cone Angle", Trans. ASME, Eng. for Ind., Series B., vol. 86, Nov. 1964, pp. 305 - 316.
2. AVITZUR, B., "Hydrostatic Extrusion", ASME Paper No. 64-WA/PROD-20. To be published in Trans. Series B.
3. PRAGER, W. and HODGE, P.G., Jr.: "Theory of Perfectly Plastic Solids", Chapman and Hall Ltd., 1951.
4. SACHS, GEORGE and KENT, R. VAN HORN: "Practical Metallurgy", p. 391. Published by American Society for Metals.
5. AVITZUR, B.: "Analysis of Wire Drawing and Extrusion Through Dies of Small Cone Angle", Trans. ASME, Eng. for Ind., Series B, vol. 85, Feb. 1963, pp. 89 - 96.
6. BERESNEV, B.I.; VERESHCHAGIN, L.F.; RYABININ, Yu. N; and LIVSHITS, L.D.: "Some Problems of Large Plastic Deformations of Metals at High Pressures", Moscow, 1960. English translation by Macmillan Company, New York, 1963.
7. WISTREICH, J.G.: "Investigation of the Mechanics of Wire Drawing", Proceedings Inst. Mech. Eng. 1955, p pp. 169, 659.
8. PUGH, H. Ll. D.: "The Cold Extrusion of Metals by High-Pressure Liquid", International research in Production Engineering, 1963. pp. 394-405, ASME Publication.
9. RYABININ, Yu. N.; BERESNEV, B.I.; and DEMYASHKEVICH, B.P.: "Variation in the Mechanical Properties of Iron Deformed by High-Pressure Hydro-Extrusion", Fiz. metal. metalloved, 11, No. 4, 630 - 633, 1961.
10. BERESNEV, B.I.; VERESHCHAGIN, L.F.; and RYABININ, Yu. N.: "The Variation in the Mechanical Properties of Iron Deformed by High-Pressure Hydro-Extrusion", Fiz. metal. metalloved, 7, No. 2, 247 - 253, 1959.

REFERENCES (Cont'd)

11. YANG, C.I.: "The Upper Bound Solution as Applied to Three-Dimensional Extrusion and Piercing Problems", Journal of Engineering for Industry, vol. 84, series B, No. 4, Nov. 1962, pp. 397 - 404.
12. AVITZUR, B.; SORTAIS, H.C.: "Experimental Study of Hydrostatic Extrusion", approved for publication in the Trans. of ASME.

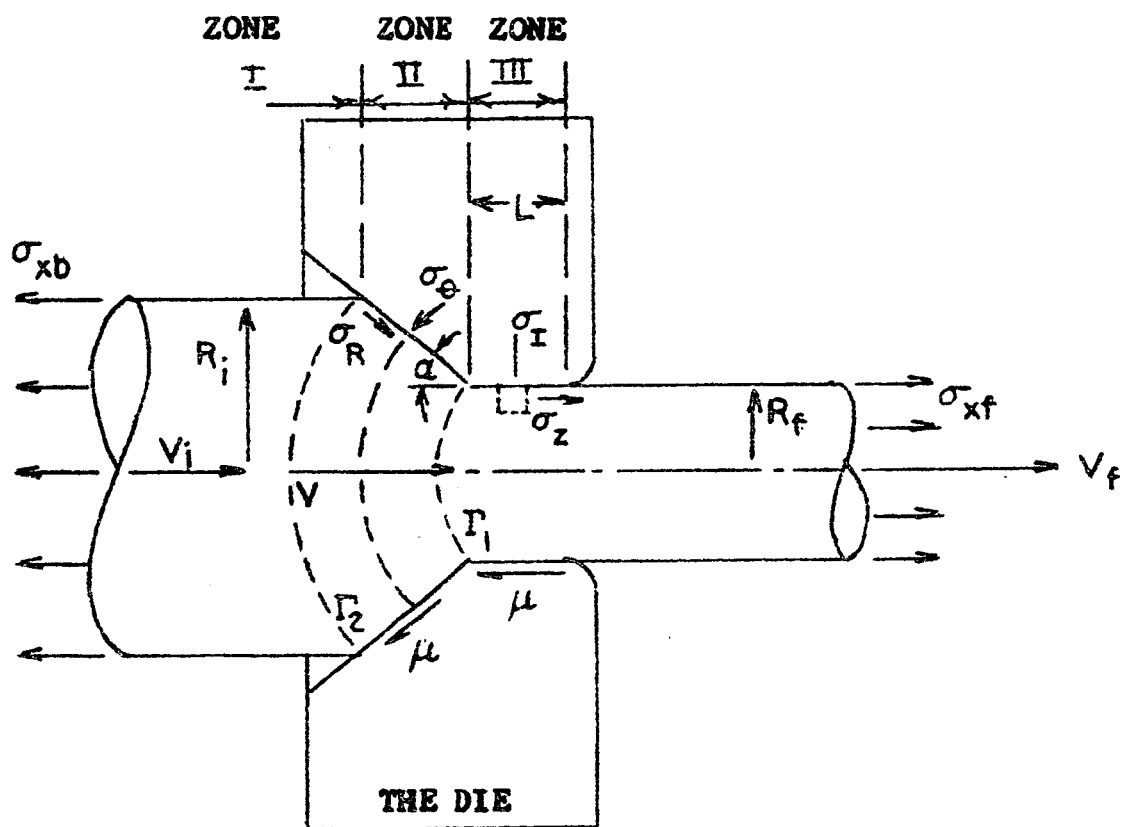


Figure 1: The die and wire in wire drawing and extrusion.

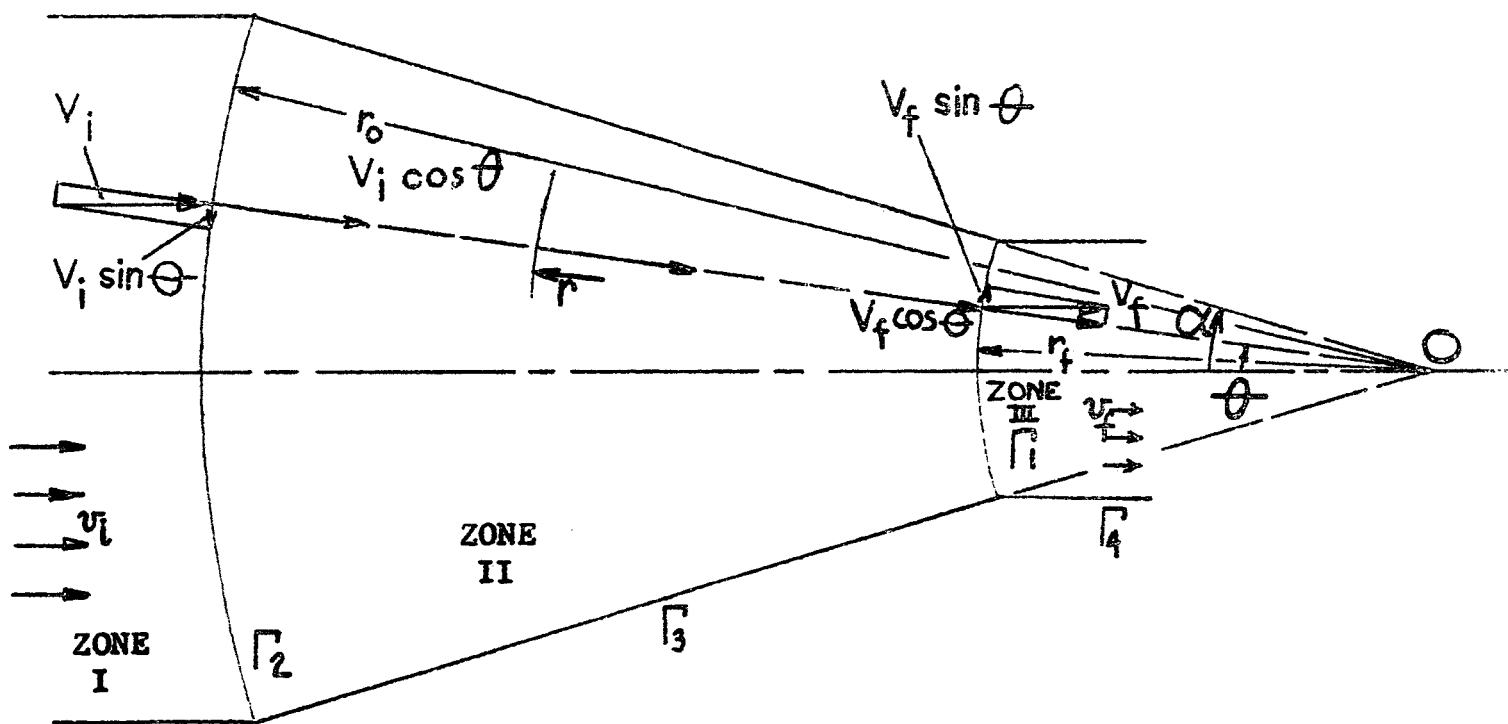


FIGURE 2: A KINEMATICALLY ADMISSIBLE VELOCITY FIELD

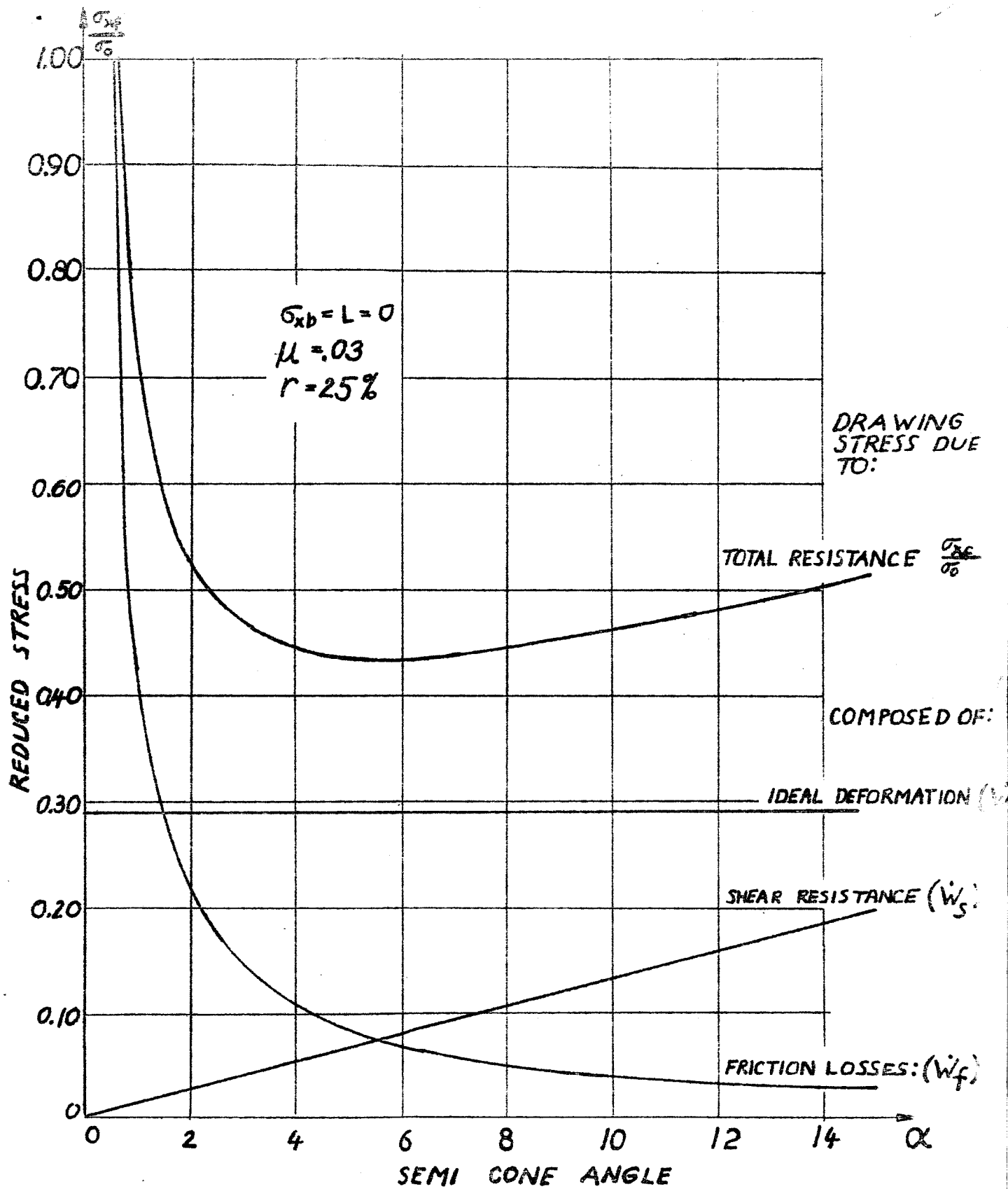


Fig. 3: Portions of the drawing stress to overcome resistance.

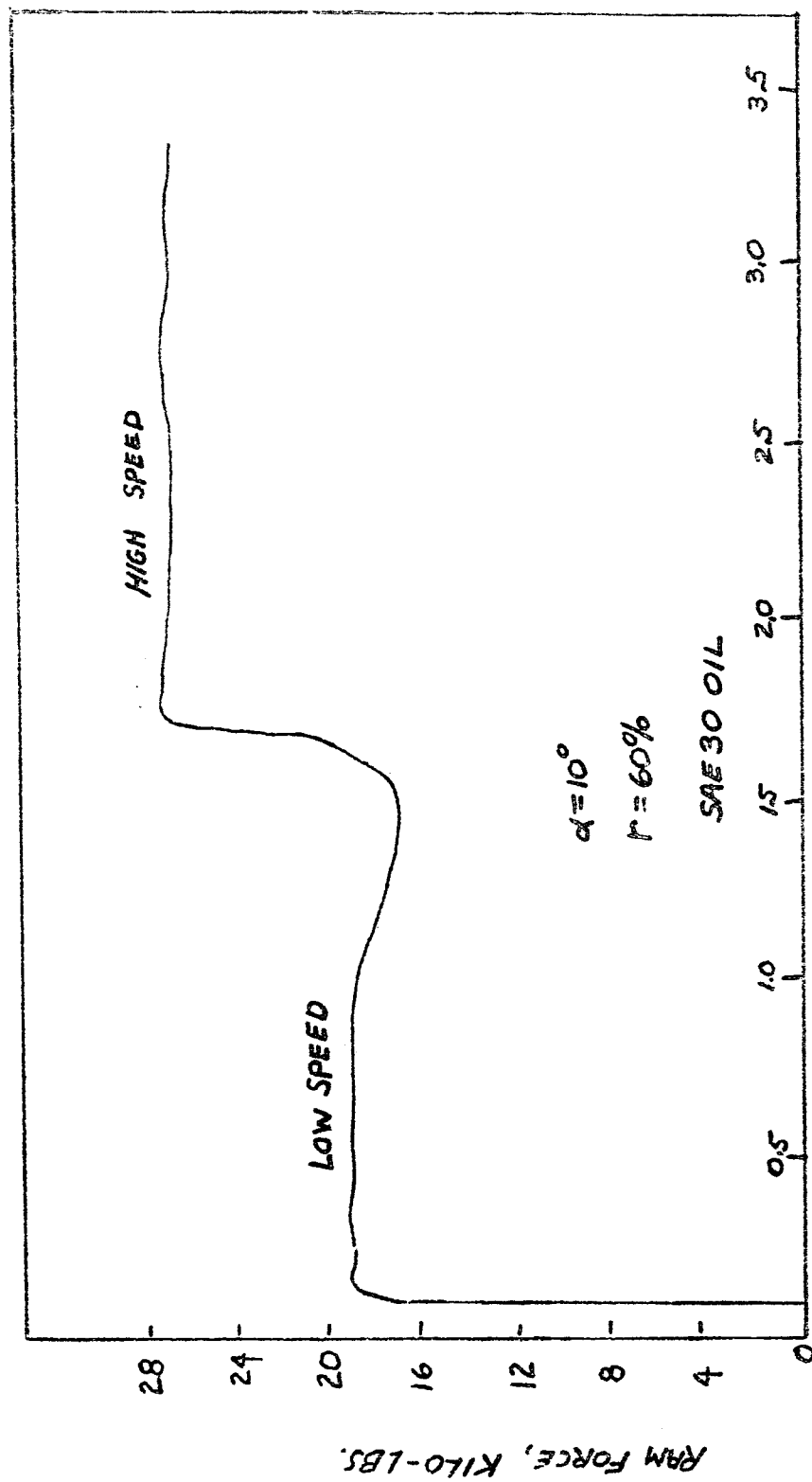
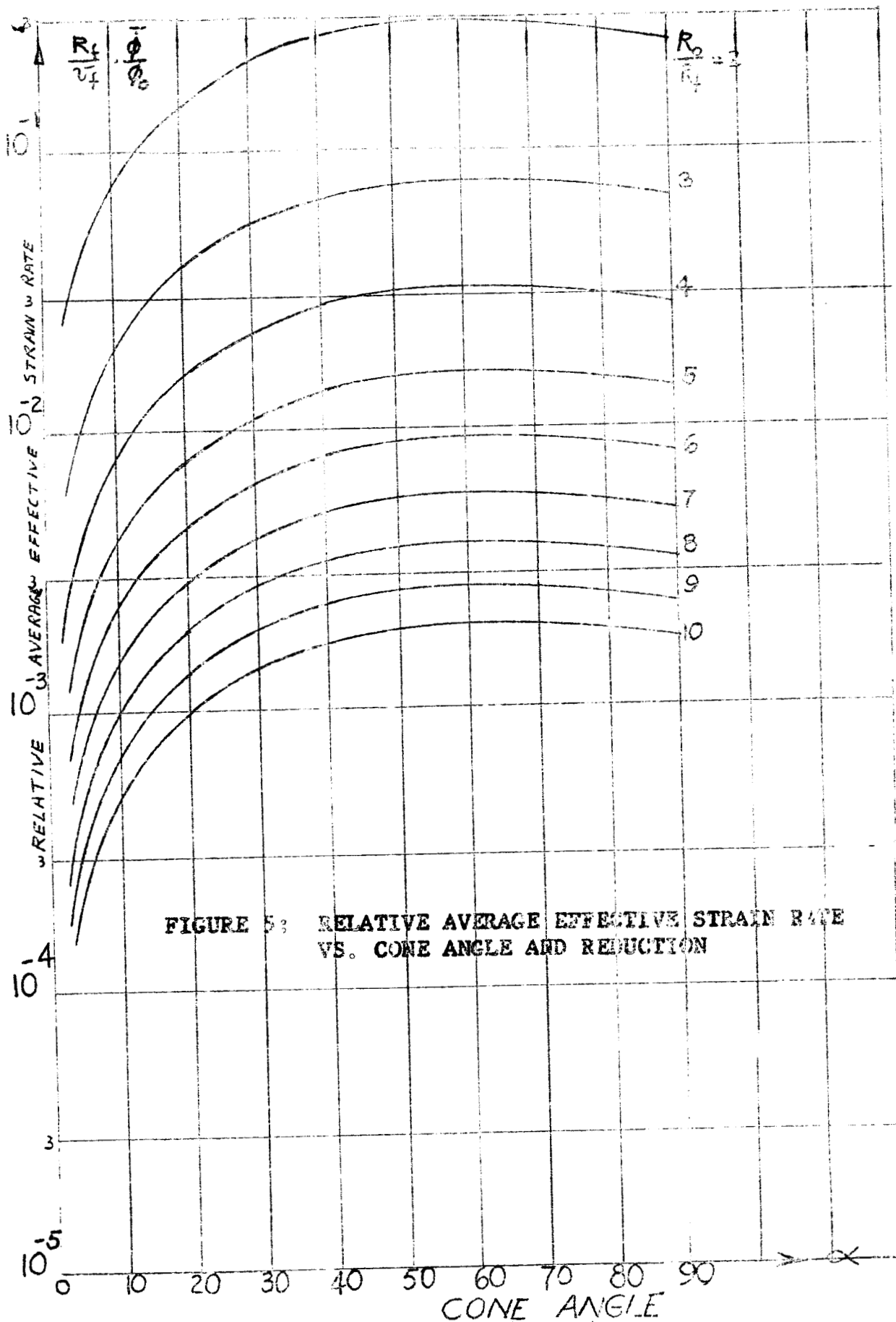


FIGURE 6: SPEED EFFECT ON EXTRUSION PRESSURE



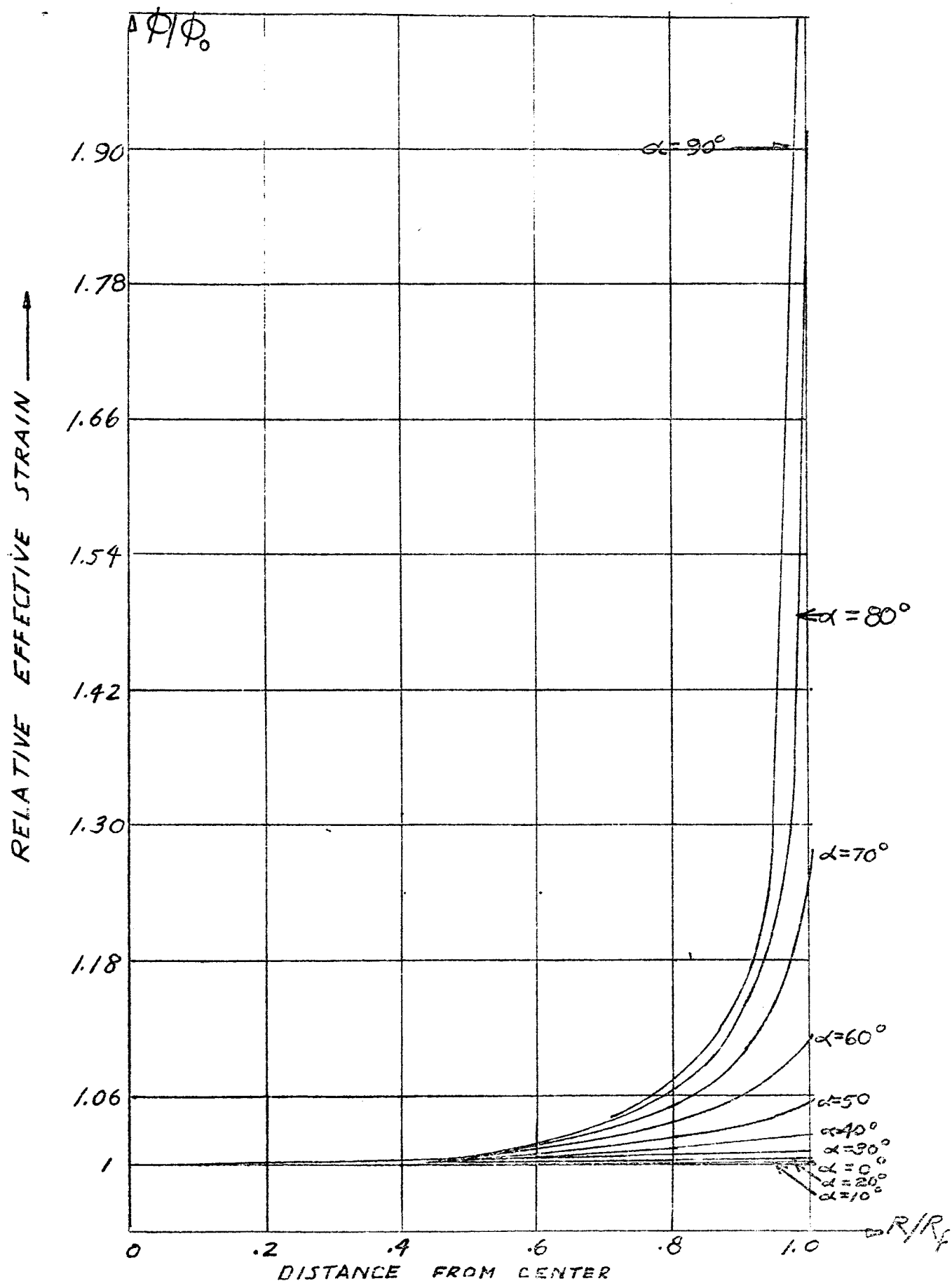


FIGURE 4b: RELATIVE EFFECTIVE STRAIN DISTRIBUTION IN FINAL PRODUCT

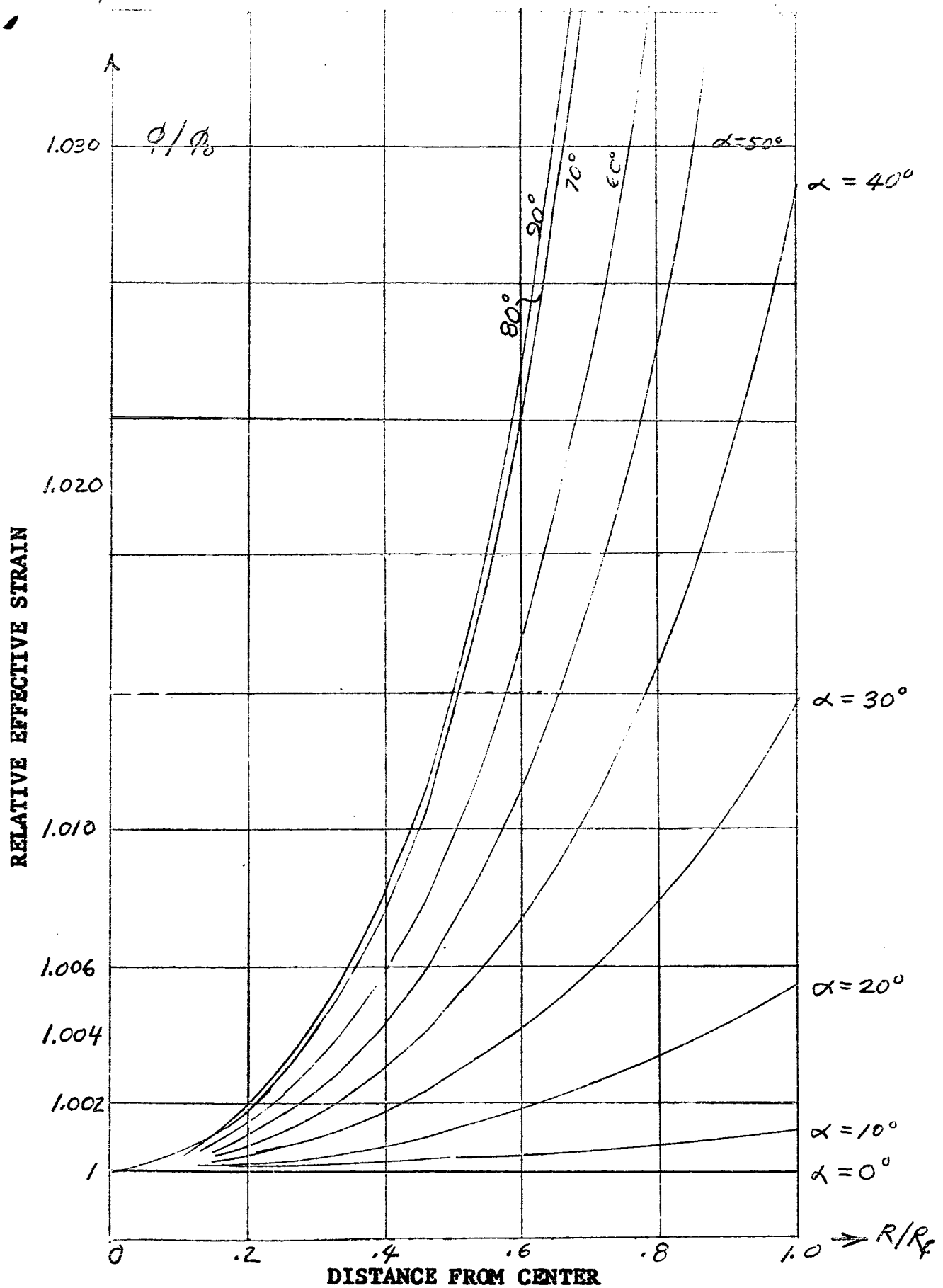


FIGURE 4a: RELATIVE EFFECTIVE STRAIN DISTRIBUTION IN FINAL PRODUCT